Intense Cr:forsterite-laser-based supercontinuum source

Ludovit Haizer,[1,2,*] Ignac Bugar,[2,3] Evgeny Serebryannikov,[4,5] Dusan Lorenc,[2] Frantisek Uherek,[2] Eleftherios Goulielmakis,[6] and Aleksei Zheltikov[4,5,7]

[1]*Department of Experimental Physics, Faculty of Mathematics Physics and Informatics, Comenius University, 842 48 Bratislava, Slovakia*

[2]*International Laser Centre, Ilkovičova 3, 84104 Bratislava, Slovakia*

[3]*Photonics Institute, Vienna University of Technology, Gußhausstraße 25-29, 1040 Vienna, Austria*

[4]*International Laser Center, Physics Department, M.V. Lomonosov Moscow State University, Vorob'evy gory, 119992 Moscow, Russia*

[5]*Russian Quantum Center, ul. Novaya 100, Skolkovo, Moscow Region 143025, Russia*

[6]*Max-Planck-Institut für Quantenoptik, Hans-Kopfermann-Strasse 1, D-85748 Garching, Germany*

[7]*Department of Physics and Astronomy, Texas A&M University, College Station, Texas 77843, USA*

**Corresponding author: haizer@ilc.sk*

Received July 4, 2014; revised August 28, 2014; accepted August 28, 2014;
posted August 29, 2014 (Doc. ID 215199); published September 19, 2014

Supercontinuum pulses covering the range from 1100 to 1700 nm with energies >1.0 mJ and excellent beam quality are generated via nonlinear spectral broadening of Cr:forsterite (1240 nm, 110 fs) pulses in pressurized molecular nitrogen. Our spectra, which extend over more than half an octave, offer an attractive alternative to intense few-cycle pulse synthesis in the 1–2 μm range and lend themselves as an important add-on to Cr:forsterite laser technologies. © 2014 Optical Society of America

OCIS codes: (320.5520) Pulse compression; (320.6629) Supercontinuum generation; (320.7120) Ultrafast phenomena; (190.7110) Ultrafast nonlinear optics; (290.5860) Scattering, Raman.
http://dx.doi.org/10.1364/OL.39.005562

Nonlinear spectral broadening of intense lasers in gaseous media to octave or superoctave bandwidths, has been a key to generating powerful few-cycle or subcycle light pulses [1,2] spanning the visible, the near infrared, and the deep ultraviolet regions of the electromagnetic spectrum. Such pulses have offered a great range of possibilities for controlling atomic and molecular phenomena [3–5] on an ultrafast time scale and lend themselves as important tools for the development of coherent EUV or soft x-rays attosecond sources [6,7].

While Ti:sapphire lasers still dominate ultrafast optical technologies, much effort is currently focused on extending few-cycle sources to longer wavelengths, toward the 1–2 μm range and beyond, as a part of the quest for efficient synthesizers of atto- and zeptosecond pulses [8] and new technologies for standoff detection [9,10]. So far, the progress in this direction has been possible due to optical parametric amplification with a solid-state laser as a front end [11]. Here, we present an alternative and in many respects, attractive approach for efficient generation of millijoule-scale supercontinuum pulses in the 1–2 μm spectral range, compressible to few-cycle pulse duration. This approach is based on the spectral broadening of Cr:forsterite laser pulses in pressurized molecular gases. Cr:forsterite lasers are capable of routinely delivering sub-30 fs light pulses centered at 1.25 μm right at the output of a mode-locked master oscillator [12,13]. Cr:forsterite amplification technologies allow millijoule-level radiation energies to be achieved in sub-100 fs pulse widths [14].

The methodology of Cr:forsterite-laser-based supercontinuum generation demonstrated in this work combines the enhanced nonlinearity of pressurized gasses [7,15], Raman scattering by molecular modulators [16–19], and the advantageous spectral centering of Cr:forsterite laser radiation allowing millijoule-level supercontinuum pulses with spectra spanning from 1.1 to 1.7 μm to be generated with an excellent beam quality. Numerical simulations based on the generalized Schrödinger equation shed light on the underlying pulse propagation dynamics, by reproducing key trends of our experimental data and suggesting temporal compressibility of the emerging supercontinua to few-cycle pulse widths.

Our laser system consists of a femtosecond oscillator, a regenerative, and two multipass amplification stages, and it delivers pulses with energy up to 4 mJ with a duration of ~110 fs at a repetition rate of 50 Hz. The pulse broadening unit is comprised of a pressurized (1–70 bar) nitrogen gas cell similar to the one introduced in Ref. [20]. The front and output fused-silica windows had a thickness of ~2 mm. The laser beam, the diameter of which was adjusted by an aperture placed before the pressurized unit, was focused around the center of the ~34 cm long cell by a thin lens ($f = 30$ cm). The distance of the lens from the entrance window was chosen to minimize nonlinear pulse broadening of the input beam. The nonlinearly transformed beam was monitored at the exit of the gas cell by NIR CCD camera, which sampled the beam profile (Xenics Xeva-1.7-320), and a NIR spectrometer (Ocean Optics NIR-512) operating both in the spectral range of 0.9–1.7 μm. Synchronized acquisition of camera and spectrometer to the laser source enabled capturing beam profiles and nonlinear spectra in the single shot regime. In order to explore conditions of optimal spectral broadening, we experimentally studied the nonlinear propagation of our pulse in the gas cell, as a function of various parameters, such as the input energy (controlled by an aperture), and the N_2 pressure. As we were primarily interested in supercontinuum pulses with a good beam quality suitable for practical applications, we have focused our study on identifying conditions for which single filament generation is attained in the cell.

In a first set of experiments, we fixed the pressure of N_2 in the cell to the maximum value attainable with our

setup (~70 bar), and studied the dependence of the spectral width, energy, and profile of the transmitted beam on the variation of the energy of the input pulses. Figure 1 summarizes results of this study. A highly asymmetric spectral broadening, manifested by a wide spectral lobe at wavelengths longer in comparison to the original spectrum, occurred at input energies of ~0.5 mJ (red/dash line) and extended to longer wavelengths as the energy increased. Intensity-uniform (within 10 dB) spectra were attained for an input energy of 1.2 mJ (blue line) and extended from 1.1 to 1.6 μm, suggesting an efficient underlying broadening mechanism. The smooth beam profile sampled for that input pulse energy setting (inset) attests to this conclusion. For $E > 1.2$ mJ, the beam quality quickly deteriorated, suggesting the onset of multiple filamentation. This deterioration of the beam quality (Fig. 1, red/dash and blue line) was also accompanied by a corresponding drop of the energy transmitted through the gas cell, as well as a narrowing of the supercontinuum spectra in relation to $E \sim 1.2$ mJ.

As a next step in our study, we explored the dependence of the properties of the emerging supercontinuum pulses on the gas pressure by keeping the input pulse energy constant. The study was performed for all input energy settings shown in Fig. 1. Here, we present data for $E = 1.2$ mJ, i.e., the energy setting for which best combination of broad bandwidth, beam quality, and output energy were achieved. Figure 2 shows spectra and beam profile dependence on the increase of the N_2 pressure. Maximum spectral width was attained at 70 bar, giving rise to supercontinuum pulses spectrally covering the range from 1.1 to 1.7 μm with energy of >1 mJ and excellent beam profile. The red-side extension of the spectra in comparison to the broadest spectra of the energy dependence (Fig. 1) was achieved by optimization of the input linear chirp of the pulses. The length of the compressor arm after the amplification process was adjusted in order to induce the maximum output bandwidth in conditions of the optimal pulse energy (1.2 mJ).

To gain insight into the physics underlying the broadening of Cr:forsterite laser in pressurized N_2, we

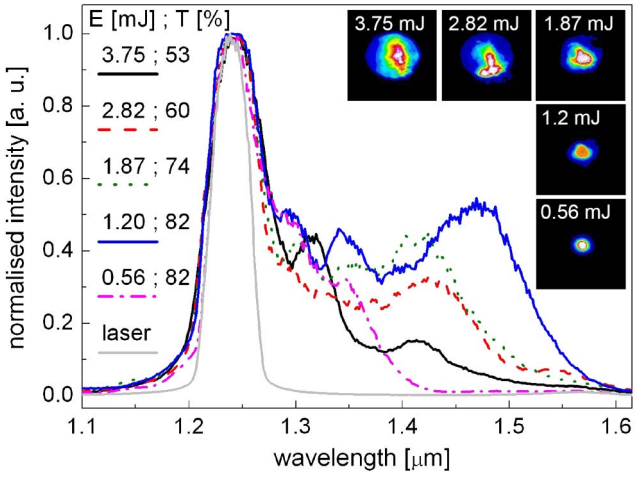

Fig. 1. Supercontinuum generation by a Cr:forsterite laser in a pressurized (70 bar) gas cell. Spectra and beam profiles of the emerging pules are shown for various setting of the input energy, controlled by an aperture.

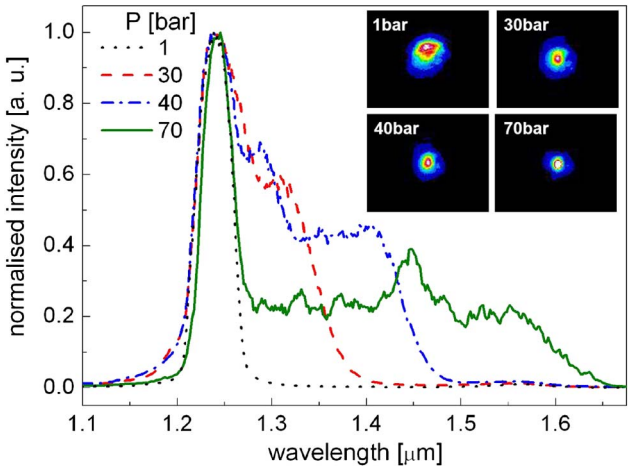

Fig. 2. Pressure dependence of the supercontinuum spectra and beam profile (insets) taken at an input energy of 1.2 mJ.

performed numerical simulation of the nonlinear broadening under conditions of our experiments. In numerical simulations, we use a model [15,21,22] based on the field evolution equation that includes the key physical effects, such as dispersion of the medium, beam diffraction, optical nonlinearities due to the cubic and higher-order susceptibilities of a gas medium, ionization-induced nonlinearities, pulse self-steepening, spatial self-action phenomena, as well as plasma loss, refraction, and dispersion. This equation is solved jointly with the equation for the electron density, where the photoionization rate W is calculated using the Popov–Perelomov–Terentyev version of the Keldysh formalism [21–23]. Parameters of the laser field and gas medium used in simulations are chosen in such a way as to model our experiments presented below. Calculations were performed with a standard set of parameters defining the ultrafast nonlinear response of high-pressure nitrogen with: Kerr nonlinearity coefficients $n_2 \approx 1.5 \times 10^{-19}(p/p_0)$ cm^2/W and $n_4 \approx -2 \times 10^{-33}(p/p_0)$ cm^4/W^2 (p is the gas pressure and p_0 is the atmospheric pressure), ionization potential $U_0 \approx 15.6$ eV, neutral gas density $\rho_0 \approx 2.7 \times 10^{19}(p/p_0)$ cm^{-3}, and a standard damped-oscillator Raman response function for molecular nitrogen.

The supercontinuum spectra calculated with the use of our model (Fig. 3) agree well with experimental results, allowing us to identify the key physical processes and scenarios whereby Cr:forsterite laser pulses generate supercontinuum in a high-pressure molecular gas. The laser beam focused into a high-pressure gas cell filled with molecular nitrogen at $p = 70$ bar induces a filament where the FWHM beam diameter remains almost constant, $d_f \approx 100$ μm, within a total length of 12 cm inside. Filamentation of the laser beam maintains high field intensity over a large propagation length, enhancing the nonlinear transformation of the laser field. Supercontinuum generation, the most dramatic manifestation of enhanced nonlinear-optical processes in our experiments, is dominated by self-phase modulation due to the instantaneous (on the considered time scale) and inertial third-order nonlinearities, conventionally referred to as the Kerr and Raman parts of optical nonlinearity. The inertia of the third-order nonlinear response, i.e.,

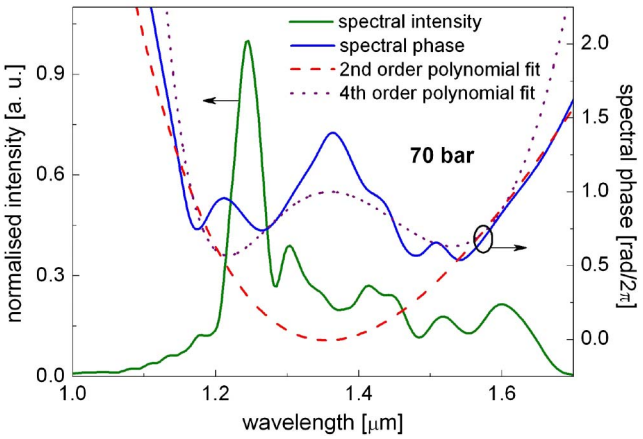

Fig. 3. Numerical modeling of supercontinuum generation in a filament induced by Cr:forsterite laser pulses with parameters as specified in the text: (green line) the spectrum and (blue line) the spectral phase of the supercontinuum output along with the (red/dash line) second-order and (purple/dot line) fourth-order polynomial fits of the spectral phase.

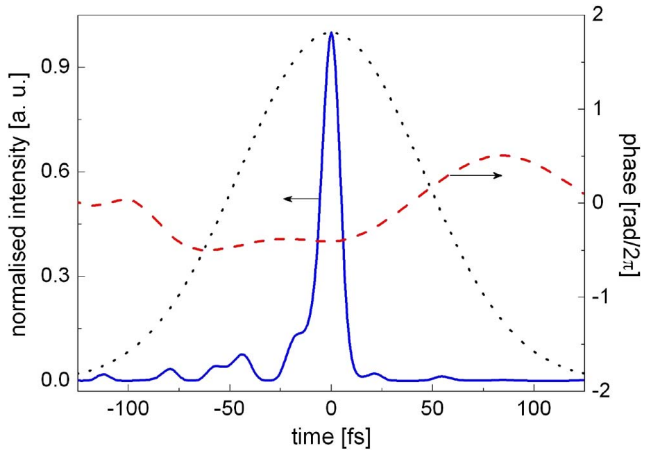

Fig. 4. Numerical modeling of pulse compression of the supercontinuum output: (black/dot line) the input pulse and (blue line) the supercontinuum output with the fourth-order phase $\varphi(4)$ (purple/dot line in Fig. 3) compensated. The red/dash line shows the residual phase of the compressed pulse following $\varphi(4)$ compensation.

the Raman effect, enhances the red wing of the supercontinuum, giving rise to asymmetric spectra and asymmetric profiles of the spectral phase at the output of the filament. This asymmetry is enhanced by ionization and self-steepening, which give rise to spectral blue shifting [15,21,22].

With the predictive power of our model confirmed by the agreement between simulations and experimental spectra, we are in a position to comment on the time-domain dynamics of the optical field waveform in the filament, although temporal pulse characterization was not performed at this stage. The supercontinuum pulse at the output of the gas cell has an FWHM pulse width close to the input pulse width. The spectral phase of this pulse is shown in Fig. 3 along with its second- and fourth-order polynomial fits, $\varphi^{(M)}(\omega) = \sum_{k=2}^{M} \alpha_j(\omega - \omega_0)^k$, where ω_0 is the central frequency and $M = 2$ and 4 for the second- and fourth-order polynomial fits, respectively. The pulse width of a transform-limited pulse supported by the entire supercontinuum spectrum produced in the filament is about 6 fs, which is less than 1.5 cycles for the central wavelength of our supercontinuum field, $\lambda_{sc} \approx 1.36$ μm. Compensation of the quadratic phase $\varphi^{(2)}$ of the supercontinuum output only with $\alpha_2 \approx 130$ fs^2 (red line in Fig. 3) yields a pulse with an FWHM pulse width $\tau_{FWHM} \approx 13$ fs. A more accurate, fourth-order phase compensation with $\alpha_2 \approx -350$ fs^2, $\alpha_3 \approx 90$ fs^3, and $\alpha_4 \approx 730$ fs^4 (purple/dot line in Fig. 3), which can be implemented using properly designed state-of-the-art chirped mirrors [24], gives a 2.2-cycle pulse with $\tau_{FWHM} \approx 10$ fs (blue line in Fig. 4) containing 42% of the input pulse energy. This pulse is preceded by a weak prepulse, which contains less than 6% of the input pulse energy, indicating a remarkably high throughput of pulse compression.

The results presented above highlight the potential of filamentation scenarios for a high-compression-ratio compression of amplified Cr:forsterite laser pulses to few-cycle pulse widths with an extraordinarily high throughput from the input pulse to the compressed waveform. Pulses that can be produced with the use of this approach are almost an order of magnitude shorter than the pulses attainable with the state-of-the-art Cr:forsterite amplifiers, opening a route toward a further integration of Cr:forsterite laser technology into the arsenal of ultrafast optical science. The maximum spectral bandwidths achieved in our experiments are typical of supercontinua generated in the filamentation regime, as reported in an extensive literature on filamentation induced by Ti: sapphire laser pulses (see, e.g., Refs. [21] and [22] for review). However, due to the λ^2 scaling of the critical power of self-focusing with the central wavelength of the driver λ, the maximum energy of supercontinuum attainable in a single Cr:forsterite-laser-induced filament with the beam still remaining stable against multiple filamentation is more than two times higher than the typical maximum energy of supercontinuum per single filament induced by Ti:sapphire laser pulses. With highly nonlinear fibers, on the other hand, the mode-locked Cr:forsterite laser output can be transformed into much broader, multioctave supercontinua [25]. However, the energy of such multioctave supercontinua is orders of magnitude lower than the energy of supercontinuum radiation in filamentation experiments presented in this work.

In conclusion we demonstrated supercontinuum generation using amplified Cr:forsterite laser pulses, yielding millijoule-level pulses with spectra spanning from 1.1 to 1.7 μm and an excellent beam quality. Such a supercontinuum source offers an important add-on to the available Cr:forsterite laser technologies [12–14] and bridges the gap between near-IR supercontinuum sources driven by standard Ti:sapphire lasers [21,22] and mid-IR supercontinua produced by high-power optical parametric chirped-pulse amplifiers using ytterbium lasers as a front end [26,27]. For many strongly scattering biological tissues, including brain, penetration depths provided by light pulses in the 1.1–1.7-μm range are larger than the penetration depths attainable with 800 nm Ti:sapphire laser pulses [28,29]. This suggests new approaches

for bioimaging [30] and neurophotonics [28,31]. Since most of the technologically significant semiconductor materials are strongly absorptive within the spectral range covered by Ti:sapphire lasers, but become transparent within the 1.1–1.7-μm range, filamentation-assisted compression of the supercontinua driven by Cr:forsterite lasers to few-cycle pulse widths could provide a unique tool for time-resolved studies of ultrafast processes in a broad class of semiconductors [14] and enable online diagnostics of electric currents in silicon integrated circuits [32].

The authors are grateful to F. Krausz, J. Fülöp, and A. Apolonskiy for their invaluable help and stimulating discussions. The work was supported in part by the Russian Foundation for Basic Research (Projects Nos. 13-02-01465, 13-02-92115, and 13-04-40335), the Welch Foundation (Grant No. A-1801), the Russian Science Foundation (Project No. 14-12-00772), the European Research Council (Attoelectronics-258501), the Deutsche Forschungsgemeinschaft (Cluster of Excellence: Munich Centre for Advanced Photonics, www.munich-photonics.de), and by the Slovak Scientific Grant Agency (Projects Nos. VEGA 1/1187/12 and VEGA 1/0907/13). Research of EES is supported by the Russian Quantum Center fellowship.

References

1. M. Nisoli, S. De Silvestri, O. Svelto, R. Szipöcs, K. Ferencz, C. Spielmann, S. Sartania, and F. Krausz, Opt. Lett. **22**, 522 (1997).
2. M. Th. Hassan, A. Wirth, I. Grguraš, A. Moulet, T. T. Luu, J. Gagnon, V. Pervak, and E. Goulielmakis, Rev. Sci. Instrum. **83**, 111301 (2012).
3. M. F. Kling, Ch. Siedschlag, A. J. Verhoef, J. I. Khan, M. Schultze, Th. Uphues, Y. F. Ni, M. Uiberacker, M. Drescher, F. Krausz, and M. J. J. Vrakking, Science **312**, 246 (2006).
4. M. F. Kling and F. Krausz, Nat. Phys. **4**, 515 (2008).
5. A. Alnaser, M. Kübel, R. Siemering, B. Bergues, N. Johnson, K. Betsch, Y. Deng, J. Schmidt, Z. Alahmed, A. M. Azzeer, J. Ullrich, I. Ben-Itzhak, R. Moshammer, U. Kleineberg, F. Krausz, R. de Vivie-Riedle, and M. F. Kling, Nat. Commun. **5**, 3800 (2014).
6. G. Sansone, E. Benedetti, F. Calegari, C. Vozzi, L. Avaldi, R. Flammini, L. Poletto, P. Villoresi, C. Altucci, R. Velotta, S. Stagira, S. De Silvestri, and M. Nisoli, Science **314**, 443 (2006).
7. E. Goulielmakis, M. Schultze, M. Hofstetter, V. S. Yakovlev, J. Gagnon, M. Uiberacker, A. L. Aquila, E. M. Gullikson, D. T. Attwood, R. Kienberger, F. Krausz, and U. Kleineberg, Science **320**, 1614 (2008).
8. T. Popmintchev, M.-C. Chen, D. Popmintchev, P. Arpin, S. Brown, S. Alisauskas, G. Andriukaitis, T. Balciunas, O. D. Mücke, A. Pugzlys, A. Baltuska, B. Shim, S. E. Schrauth, A. Gaeta, C. Hernandez-Garcia, L. Plaja, A. Becker, A. Jaron-Becker, M. M. Murnane, and H. C. Kapteyn, Science **336**, 1287 (2012).
9. D. Kartashov, S. Ališauskas, G. Andriukaitis, A. Pugžlys, M. Shneider, A. Zheltikov, S. L. Chin, and A. Baltuška, Phys. Rev. A **86**, 033831 (2012).
10. D. Kartashov, S. Ališauskas, A. Pugžlys, A. A. Voronin, A. M. Zheltikov, and A. Baltuška, Opt. Lett. **37**, 2268 (2012).
11. G. Andriukaitis, T. Balčiūnas, S. Ališauskas, A. Pugžlys, A. Baltuška, T. Popmintchev, M.-C. Chen, M. M. Murnane, and H. C. Kapteyn, Opt. Lett. **36**, 2755 (2011).
12. V. Yanovsky, Y. Pang, F. Wise, and B. I. Minkov, Opt. Lett. **18**, 1541 (1993).
13. C. Chudoba, J. G. Fujimoto, E. P. Ippen, H. A. Haus, U. Morgner, F. X. Kärtner, V. Scheuer, G. Angelow, and T. Tschudi, Opt. Lett. **26**, 292 (2001).
14. A. A. Ivanov, M. V. Alfimov, and A. M. Zheltikov, Phys. Uspekhi **47**, 687 (2004).
15. E. E. Serebryannikov, E. Goulielmakis, and A. M. Zheltikov, New J. Phys. **10**, 093001 (2008).
16. N. Zhavoronkov and G. Korn, Phys. Rev. Lett. **88**, 203901 (2002).
17. A. V. Sokolov, D. R. Walker, D. D. Yavuz, G. Y. Yin, and S. E. Harris, Phys. Rev. Lett. **85**, 562 (2000).
18. S. Baker, I. A. Walmsley, J. W. G. Tisch, and J. P. Marangos, Nat. Photonics **5**, 664 (2011).
19. A. M. Zheltikov, A. A. Voronin, R. Kienberger, F. Krausz, and G. Korn, Phys. Rev. Lett. **105**, 103901 (2010).
20. E. Goulielmakis, S. Koehler, B. Reiter, M. Schultze, A. J. Verhoef, E. E. Serebryannikov, A. M. Zheltikov, and F. Krausz, Opt. Lett. **33**, 1407 (2008).
21. L. Bergé, S. Skupin, R. Nuter, J. Kasparian, and J. P. Wolf, Rep. Prog. Phys. **70**, 1633 (2007).
22. A. Couairon and A. Mysyrowicz, Phys. Rep. **441**, 47 (2007).
23. L. V. Keldysh, Zh. Eksp. Teor. Fiz. **47**, 1945 (1964) [Sov. Phys. JETP **20**, 1307 (1965)].
24. V. Pervak, O. Pronin, O. Razskazovskaya, J. Brons, I. B. Angelov, M. K. Trubetskov, A. V. Tikhonravov, and F. Krausz, Opt. Express **20**, 4503 (2012).
25. D. A. Akimov, A. A. Ivanov, M. V. Alfimov, S. N. Bagayev, T. A. Birks, W. J. Wadsworth, P. St. J. Russell, A. B. Fedotov, V. S. Pivtsov, A. A. Podshivalov, and A. M. Zheltikov, Appl. Phys. B **74**, 307 (2002).
26. D. Kartashov, S. Ališauskas, A. Pugžlys, A. Voronin, A. Zheltikov, M. Petrarca, P. Béjot, J. Kasparian, J.-P. Wolf, and A. Baltuška, Opt. Lett. **37**, 3456 (2012).
27. D. Kartashov, S. Ališauskas, A. Pugžlys, A. Voronin, A. Zheltikov, M. Petrarca, P. Béjot, J. Kasparian, J.-P. Wolf, and A. Baltuška, Opt. Lett. **38**, 3194 (2013).
28. N. G. Horton, K. Wang, D. Kobat, C. G. Clark, F. W. Wise, C. B. Schaffer, and C. Xu, Nat. Photonics **7**, 205 (2013).
29. K. Welsher, S. P. Sherlock, and H. Dai, Proc. Natl. Acad. Sci. USA **108**, 8943 (2011).
30. B. E. Bouma, G. J. Tearney, I. P. Bilinsky, B. Golubovic, and J. G. Fujimoto, Opt. Lett. **21**, 1839 (1996).
31. L. V. Doronina-Amitonova, A. A. Lanin, O. I. Ivashkina, M. A. Zots, A. B. Fedotov, K. V. Anokhin, and A. M. Zheltikov, Appl. Phys. Lett. **99**, 231109 (2011).
32. K. A. Serrels, E. Ramsay, R. J. Warburton, and D. T. Reid, Nat. Photonics **2**, 311 (2008).